ISSN: 3107-6513

Research on the Effect of Jet Engine Exhaust Flow on Aircraft Aerodynamic Characteristics

The Son Nguyen[#1], Trong Son Phan[#2], Duc Dung Nguyen[#3], Le Phan[#4], Le Thanh Nguyen[#5]

 # Faculty of Aircraft – Engines, Air Force Officer's College, Khanh Hoa, Viet Nam

[1] theson20041993@gmail.com

Abstract:

This study examines the effect of engine injection airflow on the aerodynamic performance of an aircraft equipped with a multidirectional thrust-vectoring turbofan engine. Using the MiG-21 as a baseline platform, the original R11F-300 turbojet was replaced with a next-generation dual-stream engine to assess changes in aerodynamic behavior across various nozzle and horizontal-tail deflection angles. Three-dimensional thermo-aerodynamic simulations were performed in ANSYS CFX for multiple flight regimes at altitudes of 1 km and 10 km and a cruising Mach number of 0.45. The results indicate that deflected jet flow significantly modifies the surrounding pressure field, enhances or reduces effective thrust depending on the control-surface configuration, and strongly influences lift and lateral forces. Flow asymmetry, vortex formation behind deflected surfaces, and interactions between the jet plume and wake structures were clearly observed. These findings confirm that injection airflow and thrust-vectoring contribute substantially to maneuverability, especially during high-angle-of-attack or asymmetric control conditions. The study provides a basis for optimizing jet-flow control strategies for advanced high-agility aircraft.

Keywords - Thrust Vectoring; Injection Airflow; Aerodynamic Performance; CFD Simulation; Maneuverability

I. Introduction

The engine is one of the most important components and has an extremely complex structure. Research, design, and manufacture of engines require a great deal of time and substantial financial resources. Currently, aviation engines must meet a series of strict requirements, among which the most prominent is the ability to achieve super-maneuverability. Super-maneuverability is understood as the ability of an aircraft to maintain stability and control at large angles of attack outside the critical zone under high loads while still ensuring safety during combat operations. In addition, it is also the ability to change orientation relative to the airflow, allowing weapon systems to aim at targets regardless of the direction of the current trajectory [1].

At present, improving aircraft maneuverability is mainly based on the use of forward horizontal tailfins (canards) and thrust-vector control systems. These methods, whether used independently or in combination, provide effective control of the aircraft's attitude throughout the entire angle-of-attack range. Engines equipped with thrust-vector control systems bring many advantages, such as improved compactness; effective application for both single-engine and twin-engine aircraft; and the ability to adjust geometric parameters to achieve maximum thrust while ensuring stable engine operation in all flight modes.

This article examines the influence of injection airflow on the aerodynamic characteristics of the aircraft at different injection angles. To carry out the research, the authors selected the MiG-21 fighter as the reference model. The original engine of the MiG-21 is the R11F-300, which allows the aircraft to operate at a practical ceiling of H = 19 km and a maximum speed of M = 2. In this study, the engine was replaced with a new-generation twin-jet turbofan engine with multidirectional nozzle control (Figure 3), which has parameters close to those of a 5th-generation engine. The study was carried out using three-dimensional numerical thermo-aerodynamic simulations in ANSYS software.

Fig. 1. MiG-21 with an R11F-300 adjustable nozzle

One of the requirements for fifth-generation aircraft engines is the ability to fly supersonic without afterburner, which would significantly improve fuel efficiency and dynamic performance.

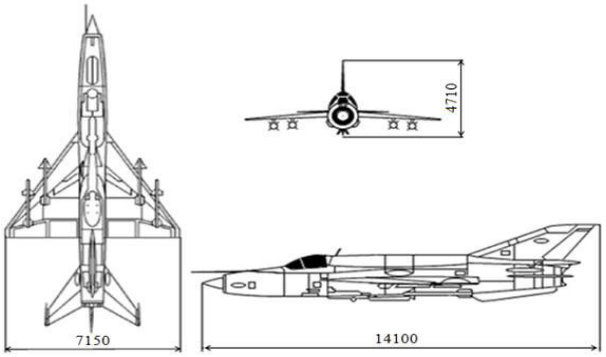

Fig. 2. MiG-21 airframe diagram

ISSN: 3107-6513

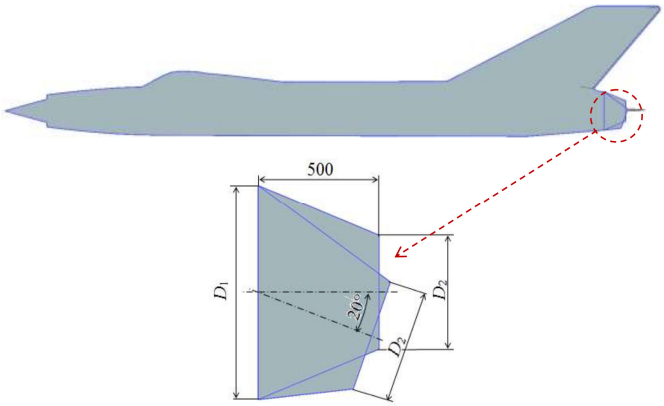

Fig. 3. Diagram of rotation of the all-aspect jet nozzle in the zero and deflected positions

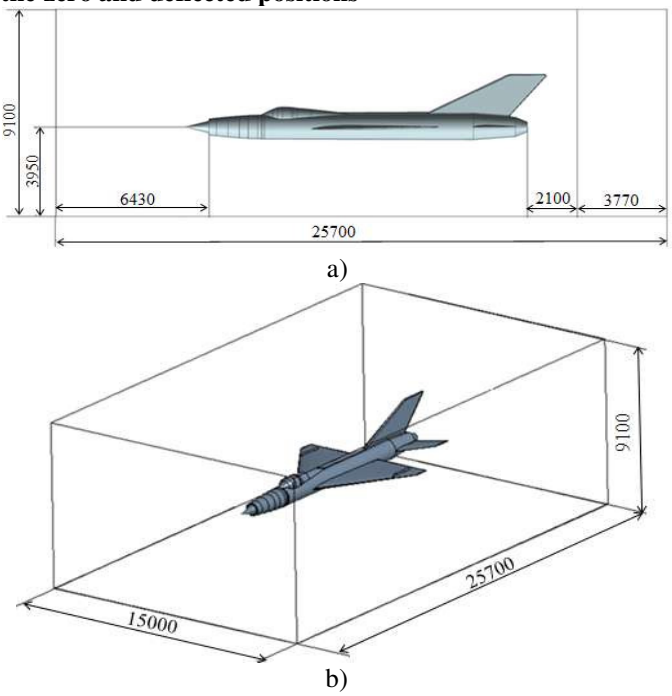

Fig. 4. Schematic diagram of the calculation model: a) side view; b) isometric view

In the study, flight regimes at the attack zone (H = 1 km) and the defense zone (H = 10 km) were considered at speed M = 0.45, with variations of the horizontal tail deflection angle as shown in Table 1:

II. Computational Meshing and Modeling

For each geometry variant, a 3D model of the fuselage and nozzle was constructed in SolidWorks (Figure 4). The model was then imported into ANSYS for meshing, boundary-condition assignment, and initialization (Figure 5).

The mesh specifications are as follows:

• Minimum cell size 35 mm in the boundary layer adhesion zone;

• Tetrahedral mesh 600 mm in the far zone;

• The supersonic jet flow zone is refined by a 32° cone truncated block, cell size 110 mm.

The total number of elements for the first variant is 5 053 274.

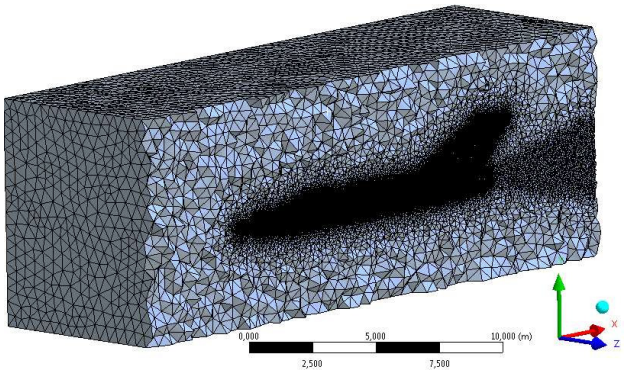

Fig. 5. Cross-sectional mesh constructed on a model with zero deflection angle of the jet nozzle (option 1)

III. Boundary conditions and simulation settings

After constructing the mesh, boundary conditions were set in CFX-Pre (Figure 6). Parameters at the critical cross-section (exit area, velocity and outlet temperature) were taken in the calculation mode (no thrust augmentation), based on the Dvigw engine simulation software [4].

In the simulation, the working medium was: Air (ideal gas); Energy model: Total Energy; Turbulence model: Shear Stress Transport (SST). Reference pressure was selected according to flight altitude.

Input conditions:

1. Inlet: Subsonic flow mode, velocity: (V_H), temperature: (T_H).

2. Opening: zero excess pressure, temperature (T_H).

3. Inlet to the gas path: Inlet condition with flow (Gv); Subsonic flow mode.

4. Nozzle outlet: Outlet condition (due to simulation according to the exit flow direction), Mixed mode, normal velocity (Vc), total temperature (T*c), residual pressure 0 Pa (simulation of full expansion).

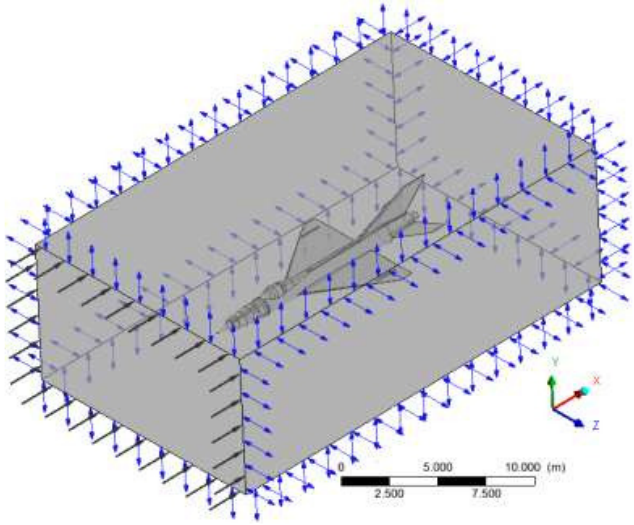

Fig. 6. Model with boundary conditions in CFX-Pre (option 1)

The input values are given in Table 2.

The calculation was run until the convergence error was less than 10^{-4} and the equation imbalance was less than 1%

ISSN: 3107-6513

Table 1. Initial data options

Option	H, km	Up-down rudder angle, degrees		Left wing Right/ wing, degrees
		Left wing	Right wing	
1 – 4	1	0	0	0; +20 up; +20 down; +20 left
5 – 9	1	-20	+20	0; +20 up; +20 down; +20 left; +20 right
10 – 13	1	-20	-20	0; +20 up; +20 down; +20 left
14 – 17	1	+20	+20	0; +20 up; +20 down; +20 left
18 – 21	10	-20	-20	0; +20 up; +20 down; +20 left

Table 2. Initial data for modeling in ANSYS CFX

Option	H, км	T_H, К	P, Pa	V_H, м/с	G_v, кг/с	Vc, м/с	T^*_c, К	F_c, м^2
1 – 4	1	281,65	89876,3	151,38	52,25	877,67	1067,83	0,1424
5 – 21	10	223,25	26499,9	134,78	21,76	963,24	1092,36	0,1718

IV. Simulation results

The simulation results are shown in Figures 7–22. Figures 9, 12, 13, and 16–22 show the velocity vector in the YZ plane at a position of 2,100 mm from the nozzle exit.

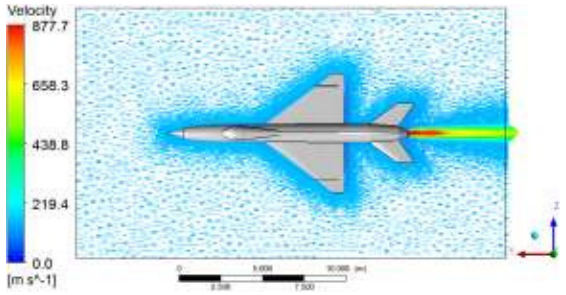

Fig. 7. Velocity vectors in the XZ plane (option 1)

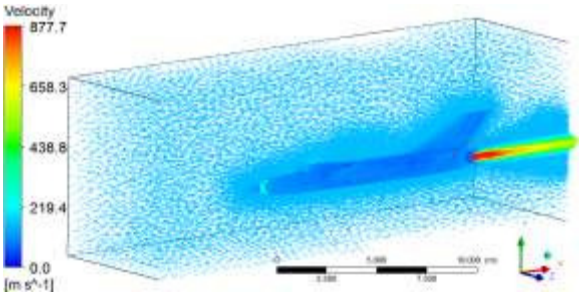

Fig. 8. 3D velocity vectors in section (option 1)

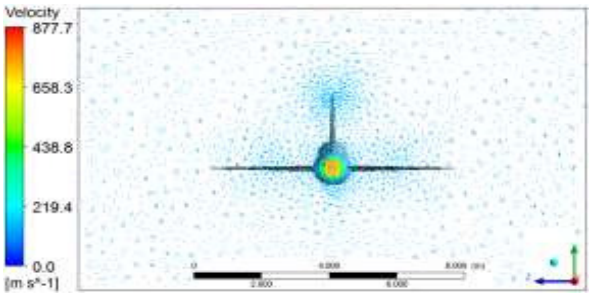

Fig. 9. Velocity vectors in the YZ plane (option 1)

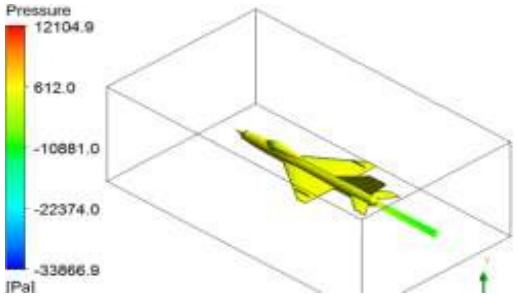

Fig. 10. Pressures acting on the airframe and flow lines exiting the nozzle (Option 1)

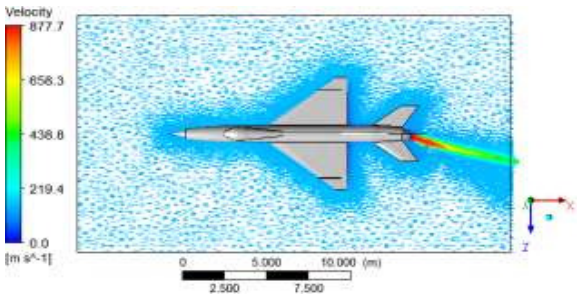

Fig. 11. Velocity vectors in the XZ plane (option 4)

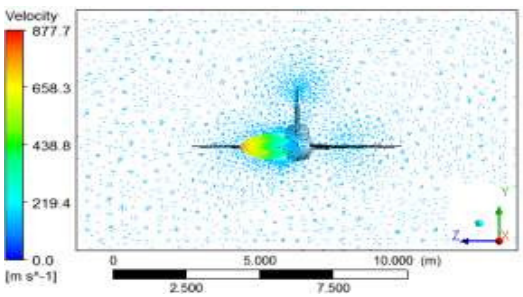

Fig. 12. Velocity vectors in the YZ plane (option 4)

ISSN: 3107-6513

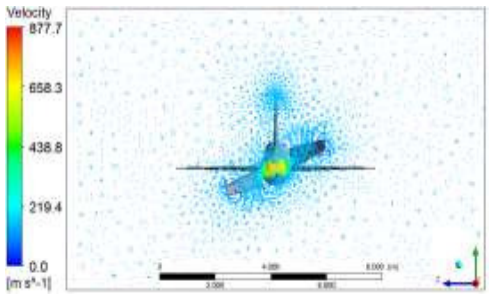

Fig. 13. Velocity vectors in the YZ plane (option 5)

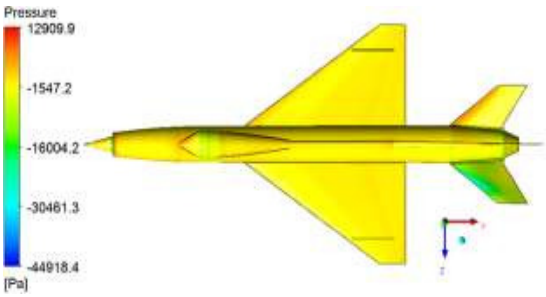

Fig. 14. Pressures acting on the airframe (Option 6)

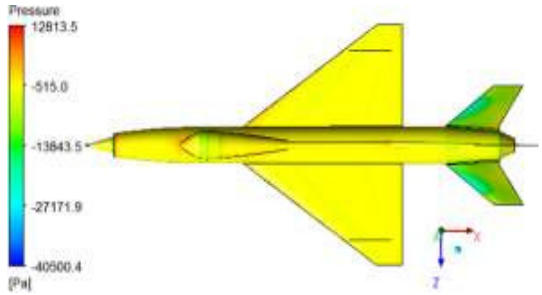

Fig. 15. Pressures acting on the airframe and flow lines exiting the nozzle (Option 11)

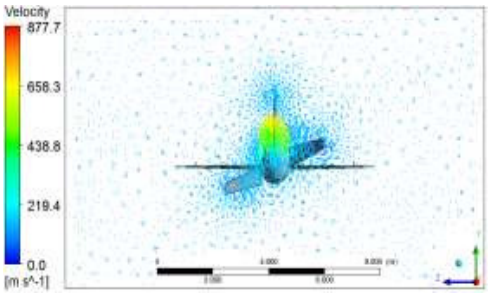

Fig. 16. Velocity vectors in the YZ plane (option 6)

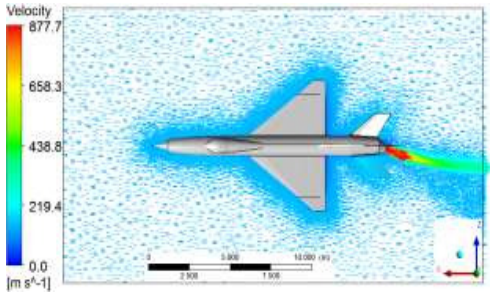

Fig. 17. Velocity vectors in the XZ plane (option 8)

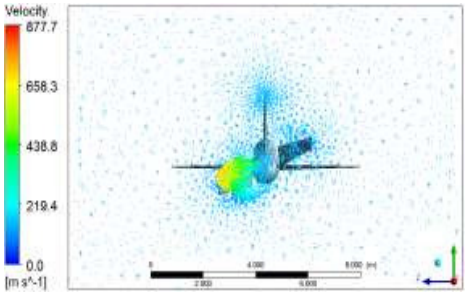

Fig. 18. Velocity vectors in the YZ plane (option 8)

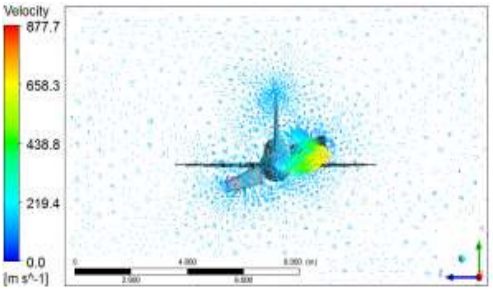

Fig. 19. Velocity vectors in the YZ plane (option 9)

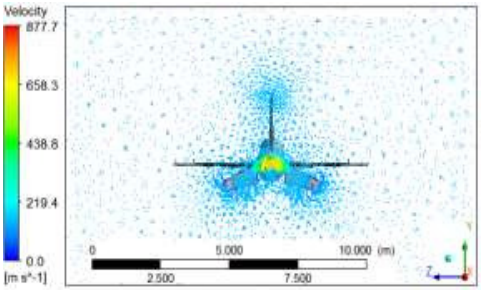

Fig. 20. Velocity vectors in the YZ plane (option 10)

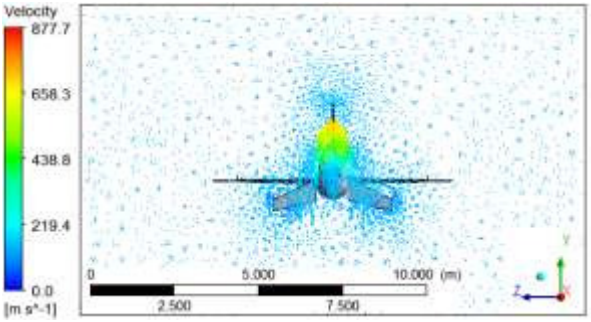

Fig. 21. Velocity vectors in the YZ plane (option 11)

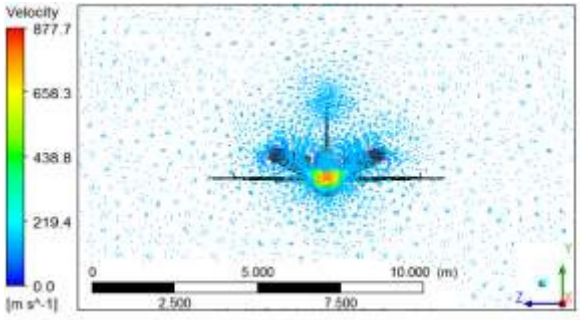

Fig. 22. Velocity vectors in the YZ plane (option 14)

ISSN: 3107-6513

V. Analysis of results

To assess the influence of the jet flow on the aerodynamic characteristics of the aircraft, for each case the authors calculated the total impulses acting on the surfaces of the computational domain. For the inlet and side surfaces, measurements were made for the impulse components perpendicular to these surfaces; for the outlet surface, measurements included all three impulse components generated by the jet flow.

The effective thrust of the engine is determined by the difference between the internal engine thrust and the total external drag [6,7]:

$$P_{engine.eff} = P_{engine} - C_x \quad (1)$$

Additionally, the effective thrust can be defined as the difference between the total impulse at the inlet face and the total impulse at the outlet face acting on two opposite faces [5]:

$$P_{engine.eff} = I_{inlet} - I_{outlet} \quad (2)$$

Sign convention: the positive direction of the total impulse coincides with the direction of the corresponding coordinate axis. If, according to calculation (2), the effective thrust has a negative value, it means that the thrust is directed opposite to the OX axis; that is, the aircraft actually has positive thrust available to continue accelerating.

In this context, the absolute values of total impulses are not decisive (because the computational domain surrounding the aircraft is chosen arbitrarily); what matters is the difference between impulses on opposite sides.

In ANSYS CFX, the total impulse values on the sides are obtained by the formula: I_inlet = force_x()@Inlet, in which the corresponding sides and components are projected onto the coordinate axes.

The obtained values for effective engine thrust $P_{\_engine.eff}$, lift ($P_{Y\Sigma}$) and lateral aerodynamic force ($P_{Z\Sigma}$) are shown in Table 3.

Table 3. Calculation results

Option	$P_{engine.eff}$, H	$P_{Y\Sigma}$, H	$P_{Z\Sigma}$, H	Phương án	$P_{engine.eff}$, H	$P_{Y\Sigma}$, H	$P_{Z\Sigma}$, H
1	-11220	463	13	12	36180	-59788	155
2	-2780	20737	-17	13	30840	-40852	-19023
3	-6980	-20988	-95	14	36000	47248	-29
4	-6270	103	-19146	15	53950	66791	-49
5	22180	-38	11701	16	35250	28043	5
6	25190	19427	11244	17	26170	41081	-20919
7	21470	-17649	11509	18	3240	-11992	-6
8	6620	2332	-7748	19	1900	-3674	-12
9	5970	-1348	30552	20	5990	-20200	58
10	31260	-44908	-61	21	1960	-12140	-8712
11	27780	-23091	90	–	–	–	–

Analysis of the calculation results

From analysis of the flow-field morphology and calculation results in non-boosting modes, the authors found that when the jet nozzle and horizontal tail deflection angles are zero, the flow pattern is symmetrical (Figure 10). In calculations with zero horizontal tail deflection, the aircraft has a positive residual thrust value (the aircraft accelerates). In other modes (when the horizontal tail deflection angle changes), the residual thrust is negative (the aircraft decelerates)—this phenomenon is related to the increase in drag caused by horizontal tail deflection. When the horizontal tail is deflected, the flow pattern around the aircraft becomes asymmetrical, with vortices appearing behind the horizontal tail (Figures 13, 20, 22).

When the jet stream is deflected, it interacts with those vortices and the flow pattern changes (Figures 16, 18, 19, 21). Changes in the distribution of residual static pressure on the fuselage surfaces are observed when the tail is deflected: on the surfaces toward which the tail is deflected, the pressure increases; on the opposite surfaces, the pressure decreases (Figs. 14 and 15). This pressure differential enables the aircraft to perform large maneuvers. In Figs. 11 and 17, and 12 and 18, the interaction between the vortex trail generated behind the deflected control surfaces and the jet stream is clearly visible.

Deformation of the vortex trail behind the horizontal and deflected tail in the supersonic airflow is observed. These phenomena can be quantitatively assessed from the results presented in Table 3. The same nozzle-deflection angle produces different effects on the aircraft depending on the horizontal tail deflection angle. Deflection of the control surfaces and jet nozzle induces rotational and torque moments acting on the fuselage. To evaluate them, it is necessary to determine the total force acting on the fuselage and the position of that force relative to the aircraft's center of mass.

Conclusion

By means of three-dimensional thermo-aerodynamic numerical simulation in the ANSYS software package, the authors studied the influence of the airflow from the jet engine nozzle on the aerodynamic characteristics of the aircraft. The simulation results allow determination of the effective engine thrust, lift force, and lateral aerodynamic force depending on the positions of the fuselage control

ISSN: **3107-6513**

elements and the jet nozzle, at flight speed M = 0.45 and altitudes of 1 km and 10 km.

REFERENCES

[1] А.В. Гарбарук, М.Х. Стрелец, М.Л. Шур (2012) “Моделирование турбулентности в расчетах сложных течений.”

[2] Л.С. Шаблий, А.В. Кривцов, Д.А. Колмакова (2017) “Компьютерное моделирование типовых гидравлических и газодинамических процессов двигателей и энергетических установок в Ansys Fluent”.

[3] Кривошеев И.А. Исследование течения в двухконтурных соплах с раздельным истечением потоков при наличии внешнего обтекания / Кривошеев И.А., Ахмедзянов Д.А., Кишалов А.Е., Маркина К.В.// Молодёжный Вестник УГАТУ Ежемесячный научный журнал – Уфа: УГАТУ. – 2013 - №2 (7). – С. 25-36.

[4] Ахмедзянов Д.А. Моделирование совместной работы авиационных ГТД и элементов топливной автоматики на переходных режимах в компьютерной среде DVIGw / Д. А. Ахмедзянов, Х. С. Гумеров, И. А. Кривошеев // Изв. вузов, сер. «Авиационная техника». – Казань, 2002. – №1. – С. 43–46.

[5] Molodchikov V.M. Issledovanie primenimosti paketa FLUENT k modelirovaniju dozvukovyh otryvnyh techenij. Teplofizika i aeromekhanika. 2009. № 3. Pp. 387-394. (In Russian).

[6] Akimov A.N., Vorob'ev V.V., Demchenko O.F., Dolzhenkov N.N., Matveev A.I., Podobedov V.A. Osobennosti proektirovaniya legkikh boevykh i uchebno-trenirovochnykh samoletov. Pod red. N.N. Dolzhenkova, V.A. Podobedova. M.: Mashinostroenie - Polet. 2005. 368 p. (In Russian).

[7] Бакулев В. И. Теория, расчет и проектирование авиационных двигателей и энергетических установок / Бакулев В. И., Голубев В. А., Крылов Б. А., Марчуков Е. Ю., Нечаев Ю. Н., Онищик И. И., Сосунов В. А., Чепкин В. М. // Издание 3-е. – МАИСАТУРН, 2003. 688 с.